Half-metallicity at the Heusler alloy $Co_2Cr_{0.5}Fe_{0.5}Al(001)$ surface and its interface with GaAs(001)

2009 J. Phys.: Condens. Matter 21 055002

(http://iopscience.iop.org/0953-8984/21/5/055002)

J. Phys.: Condens. Matter **21** (2009) 055002 (7pp) doi:10.1088/0953-8984/21/5/055002

Half-metallicity at the Heusler alloy $Co_2Cr_{0.5}Fe_{0.5}Al(001)$ surface and its interface with GaAs(001)

Sareh Zarei, S Javad Hashemifar, Hadi Akbarzadeh and Zohre Hafari

Department of Physics, Isfahan University of Technology, Isfahan 84156, Iran

E-mail: akbarzad@cc.iut.ac.ir

Received 14 May 2008, in final form 19 November 2008
Published 16 December 2008
Online at stacks.iop.org/JPhysCM/21/055002

Abstract

Electronic and magnetic properties of the Heusler alloy $Co_2Cr_{0.5}Fe_{0.5}Al(001)$ surfaces and its interfaces with GaAs(001) are studied within the framework of density functional theory by using the plane-wave pseudopotential approach. The phase diagram obtained by *ab initio* atomistic thermodynamics shows that the CrAl surface is the most stable (001) termination of this Heusler alloy. We discuss that, at the ideal surfaces and interfaces with GaAs, half-metallicity of the alloy is lost, although the CrAl surface keeps high spin polarization. The energy band profile of the stable interface is investigated and a negative p Schottky barrier of −0.78 eV is obtained for this system.

(Some figures in this article are in colour only in the electronic version)

1. Introduction

Electrical spin injection from ferromagnetic metals into semiconductors has been an increasingly important issue in magneto-electronics studies [1]. The main obstacle to achieving efficient spin injection in these systems is the impedance mismatch in the diffusive transport regime [2]. The use of half-metallic ferromagnets has been proposed as an approach to circumvent this obstacle and obtain efficient spin injection [2]. As predicted by first-principles calculations [3], in a half-metallic compound one spin channel behaves like a metal whereas the Fermi energy is located inside the energy gap of the other channel, leading to 100% spin polarization at the Fermi level. However, in reality the half-metallic property could be lost due to any kind of crystal disorders, such as defects, surfaces and interfaces. In this regard, the study of half-metal/semiconductor junctions and corresponding surface and interface-related effects on the relevant electronic and magnetic properties of the system is an essential step towards practical applications.

Recently, the Co-based full-Heusler compounds (e.g. $Co_2Cr_{1-x}Fe_xAl$, Co_2MnSi, etc) have attracted considerable attention for spin injection applications because of their high Curie temperatures [4]. In this group Co_2CrAl shows half-metallic electronic structure with a Curie temperature of about 334 K [5]. The half-metallic character of Co_2CrAl/InP interfaces has been studied by Galanakis and a rather high degree of spin polarization, more than 50%, has been found for this interface [6]. He has also shown that the CrAl-terminated surface of $Co_2CrAl(001)$ has higher spin polarization than the Co-terminated surface [7]. Nagao *et al* have argued that spin polarization tends to remain relatively high at the Co_2CrAl/GaAs(110) interface [8]. Jakob *et al* have succeeded to improve the Curie temperature of the Co_2CrAl alloy by alloying with Fe dopant [9]. By controlling the stoichiometry of the samples, they grew the $Co_2Cr_{0.6}Fe_{0.4}Al$ alloy with a measured high Curie temperature of about 665 K. Moreover, a large room temperature magnetoresistance of about 37% in a rather small magnetic field (0.25 T) was observed in this alloy [10] whereas the Co_2CrAl compound shows no such effect.

To date, no theoretical work has been performed on $Co_2Cr_{0.6}Fe_{0.4}Al$ surfaces and its interface with semiconductors and the level of electronic state spin polarization in these systems is unknown. Hence, a first-principles electronic structure study is helpful to understand the possible surface and interface effects on the half-metallic property of $Co_2Cr_{0.6}Fe_{0.4}Al$ thin films and provide an outlook on practical

applications of this material. Due to the specific stoichiometry of Fe and Cr atoms in $Co_2Cr_{0.6}Fe_{0.4}Al$, very large supercells are required to simulate surfaces and interfaces of this compound while high symmetry $Co_2Cr_{0.5}Fe_{0.5}Al$ alloy with very close stoichiometry to the original Heusler alloy leads to much smaller supercells. Hence, we adopted this simplified Heusler alloy for our calculation.

In this paper, we present the results of our pseudopotential study on the electronic and magnetic properties of $Co_2Cr_{0.5}Fe_{0.5}Al(001)$ surfaces and interfaces with GaAs(001). In the following, after introducing our method of calculations, the surface and interface results will be discussed in two separate subsections and the summary of the results will be presented in the last section.

2. Computational method

Our calculations have been performed within the framework of spin-polarized density functional theory (DFT) [11], using the generalized gradient approximation (GGA) according to the Perdew *et al* parameterization [12]. We adopt GGA because the lattice constant of $Co_2Cr_{0.5}Fe_{0.5}Al$ (5.65 Å) calculated on the basis of GGA shows good agreement with the experimental value (5.76 Å) [13]. The calculations were performed by using the PWscf code [14], which employs the plane-wave ultrasoft pseudopotential method [15]. Spin–orbit interactions are not included. The wavefunctions were expanded in a plane-wave basis set with energy cutoff of 43 Ryd while a cutoff of 668 Ryd was used for the augmentation density of Vanderbilt pseudopotentials. The Brillouin zone (BZ) integration, has been done on a regular $(8 \times 8 \times 1)$ grid of Monkhorst–Pack k-points [16] in the irreducible wedge of the surface and interface BZ by using the Methfessel–Paxton smearing method [17] and a broadening parameter of 0.02 Ryd.

3. Results and discussions

3.1. Surface results

The cubic structure of $Co_2Cr_{0.5}Fe_{0.5}Al$ alloy, sketched in figure 1, in the (001) direction consists of three different planes; FeAl, Co and CrAl planes with the alternating sequence of −CoCo–FeAl–CoCo–CrAl− (the Co planes are named CoCo to clarify the correct stoichiometry of atoms in the plane). Therefore there are four possible (001) terminations for this alloy; two of them are FeAl and CrAl surfaces while the other two are CoCo surfaces on two different subsurface layers; FeAl and CrAl, called Co–Fe and Co–Cr throughout this paper, respectively. It should be noted that, in addition to these four ordered surface terminations, there is also one possible disordered termination; an intermixed $Fe_{0.5}Cr_{0.5}Al$ layer. Simulation of this disordered termination needs a larger supercell and is omitted in our study. The four ordered surface terminations were simulated by using symmetrical 1×1 supercells consisting of 15 (for two CoCo surfaces) or 17 (for two other surfaces) atomic layers and a 16 Bohr thick vacuum region. The vacuum thickness was optimized to prevent interaction between adjacent surfaces and the number

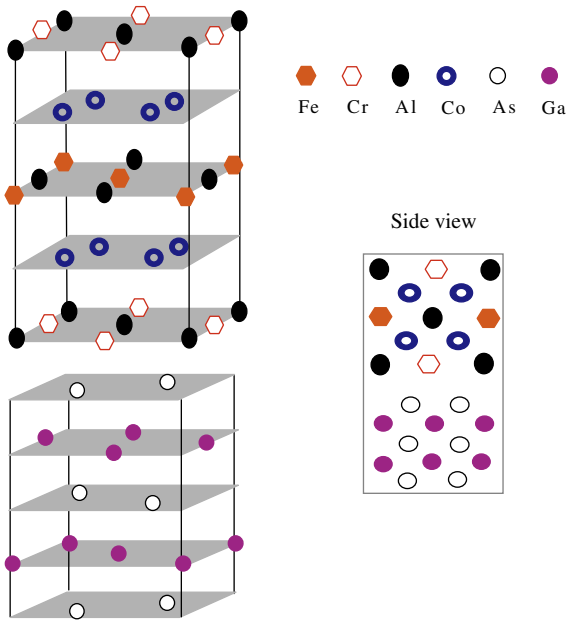

Figure 1. Schematic representation of the $Co_2Cr_{0.5}Fe_{0.5}Al(001)$ surface (CrAl termination) and its interface with GaAs(001) (CrAl/As termination).

of layers was also optimized to achieve bulk-like properties at the center of the slabs. The supercells were made symmetrical to avoid creation of slab dipoles. The total energy of all supercells was minimized by accurate relaxation of all atomic positions (except a few central layers) down to the force values of 1 mRyd/Bohr and energy accuracy of 0.1 mRyd.

The first part of our discussion addresses the relative stability of the different surfaces within the framework of *ab initio* atomistic thermodynamics [18, 19]. In this scheme, the surface free energy γ, defined as follows, is used to assess the stability of different terminations:

$$\gamma = \frac{[G(T, p_i) - \sum_i N_i \mu_i(T, p_i)]}{2A}. \quad (1)$$

Here, G is the Gibbs free energy of the surface, N_i and μ_i are the number and the chemical potential of the ith element, $2A$ is the total surface area of the symmetrical supercell and γ is the surface free energy per area. By calculating and comparing the surface free energies of different terminations in a reasonable range of the chemical potentials, one finds the stable surface having the lowest surface free energy for any given values of chemical potentials and the results of this comparison could be represented as a phase diagram.

Clearly, four chemical potentials enter the $Co_2Cr_{0.5}Fe_{0.5}Al$ surface free energies (equation (1)). But, since the calculated slabs have bulk-like central layers, their surfaces are in thermodynamic equilibrium with central bulk layers and hence the following equilibrium condition is imposed on the chemical potentials:

$$g_{\text{bulk}} = 2\mu_{\text{Co}} + 0.5\mu_{\text{Cr}} + 0.5\mu_{\text{Fe}} + \mu_{\text{Al}} \quad (2)$$

g_{bulk} is the Gibbs free energy of the bulk $Co_2Cr_{0.5}Fe_{0.5}Al$. This relation reduces the number of independent chemical potential

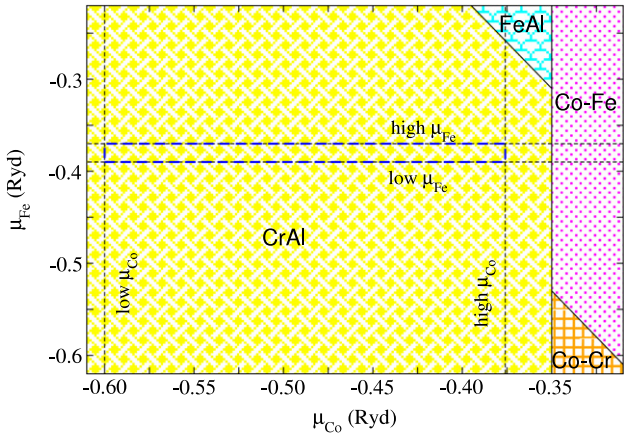

Figure 2. Phase diagram of the four ideal terminations of $Co_2Cr_{0.5}Fe_{0.5}Al(001)$. The thin dashed lines are the low and high limits of the chemical potentials and the thick dashed lines show the practically accessible region of the phase diagram.

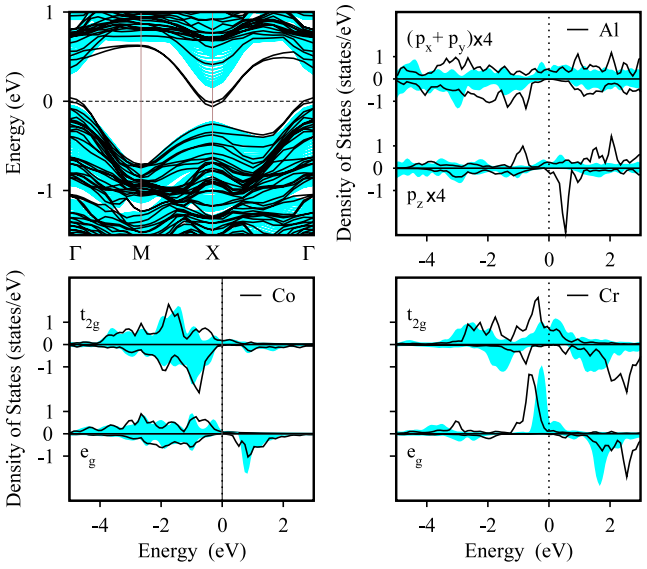

Figure 3. The minority band structure and the spin-resolved partial DOS[1] of the surface Cr and Al atoms and the subsurface Co atom at the ideal CrAl termination. The p_z and $(p_x + p_y)$ partial DOS are multiplied by 4 to aid clarity. Positive and negative DOS correspond to the majority and minority states, respectively. Shaded areas are the corresponding bulk properties. The Fermi energy is set to zero.

of equation (1) to three. Moreover, since all supercells have the same number of Al atoms, μ_{Al} has no influence on the relative stability of different surfaces and by setting it to a constant value (energy of an isolated Al atom) only two independent chemical potentials remain in the surface free energies. We selected them to be μ_{Co} and μ_{Fe} while any other choice would not change our main conclusions.

[1] Due to the tetragonal symmetry of our surface and interface supercells the atomic d partial DOS (PDOS) in these systems is split into d_{xy}, $(d_{xz} + d_{yz})$, d_{z^2}, and $d_{x^2+y^2}$. But in order to compare easily the surface and interface PDOS with bulk properties and decrease complexity of the corresponding plots, we added the d_{xy} and $(d_{xz} + d_{yz})$ PDOS together to make the t_{2g} PDOS, and the d_{z^2} and $d_{x^2+y^2}$ together to make the e_g PDOS.

The Gibbs free energy has two main contributions: the static total energy (comes out of the DFT calculations) and the vibrational energy. It is argued that at sufficiently low temperatures often the vibrational contributions can be harmlessly neglected [19] and the DFT total energies suffice for surface free energy calculations. In practice, the obtained phase diagram in this procedure is only valid within a limited range of the chemical potentials because over-increasing or-decreasing these parameters may lead to decomposition of the alloy. For example, if μ_{Fe} becomes too low then the Fe atoms prefer to leave the sample and bulk Co_2CrAl will form. Hence, the lower limit of μ_{Fe} is determined by the Gibbs free energy of the bulk Co_2CrAl:

$$g_{\text{bulk}}^{\text{Co}_2\text{CrAl}} = 2\mu_{\text{Co}} + \mu_{\text{Cr}} + \mu_{\text{Al}}. \tag{3}$$

In the same way, the other practical limits of the chemical potentials are; high μ_{Fe} ($g_{\text{bulk}}^{\text{Fe}} = \mu_{\text{Fe}}$), low μ_{Co} ($g_{\text{bulk}}^{\text{FeAl}} + g_{\text{bulk}}^{\text{CrAl}} = \mu_{\text{Fe}} + \mu_{\text{Cr}} + 2\mu_{\text{Al}}$) and high μ_{Co} ($g_{\text{bulk}}^{\text{Co}} = \mu_{\text{Co}}$).

Following the above-mentioned method we calculated the phase diagram of the $Co_2Cr_{0.5}Fe_{0.5}Al$ surfaces as a function of the cobalt and iron chemical potentials and plotted it in figure 2. Clearly the CrAl surface is found to be the most stable termination in the whole accessible region of the phase diagram.

The stability of CrAl termination could be understood by considering and comparing bond energies in $Co_2Cr_{0.5}Fe_{0.5}Al$ alloy. There are 16 Co–Cr, 16 Co–Fe, and 32 Co–Al nearest-neighbor bonds in the cubic cell of this alloy. In order to estimate the energy of these three kinds of bonds we split the bulk $Co_2Cr_{0.5}Fe_{0.5}Al$ alloy into three groups of sublattices: $(Co_2Fe_{0.5}Al + Cr_{0.5})$, $(Co_2Cr_{0.5}Al + Fe_{0.5})$ and $(Co_2Cr_{0.5}Fe_{0.5} + Al)$. Then the total energies of all these six sublattices were calculated and compared to the bulk energy (E_{tot}) to estimate the corresponding bond energies as follows:

$$E_{\text{Co-Cr}} = 1/16(E_{\text{tot}} - E_{\text{Co}_2\text{Fe}_{0.5}\text{Al}} - E_{\text{Cr}_{0.5}}) \tag{4}$$

$$E_{\text{Co-Fe}} = 1/16(E_{\text{tot}} - E_{\text{Co}_2\text{Cr}_{0.5}\text{Al}} - E_{\text{Fe}_{0.5}}) \tag{5}$$

$$E_{\text{Co-Al}} = 1/32(E_{\text{tot}} - E_{\text{Co}_2\text{Cr}_{0.5}\text{Fe}_{0.5}} - E_{\text{Al}}). \tag{6}$$

We found that the energies of Co–Cr, Co–Fe, and Co–Al bonds are about 0.60 eV, 0.43 eV and 0.17 eV, respectively. This qualitative comparison indicates stronger interaction between CrAl surface and CoCo subsurface layers compared with the FeAl surface, evidence for more stability of the CrAl termination.

In order to study the electronic structure of $Co_2Cr_{0.5}Fe_{0.5}Al(001)$ surfaces, we calculated the spin-polarized band structure and density of states (DOS) of all terminations. The obtained results for the stable CrAl surface is shown in figure 3. We observed that in all cases some surface states appearing in the bulk half-metallic gap destroy the half-metallicity of the system and reduce the Fermi level spin polarization from the ideal 100% value. However, as is evident in the figure, the CrAl surface states inside the half-metallic gap have low density and hence a rather high degree of spin polarization was calculated at the Fermi level of this system (77%), larger than those of the other three surfaces. Moreover, obviously no surface states cross from the valence band into the conduction

band; rather, the valence and conduction bands are separated and a true indirect gap between Γ and X is just missed. Perhaps a more correct treatment of exchange–correlation effects can open this gap by pushing up the conduction band at X. A different exchange–correlation treatment can be given by the LDA + U method. Galanakis studied (001) surfaces of a similar Heusler alloy Co_2CrAl and found a spin polarization of about 84% at the CrAl termination of this alloy [6]. But an important point is the effect of atomic relaxation at surfaces, which is not considered in the work of Galanakis. In the case of $Co_2Cr_{0.5}Fe_{0.5}Al(001)$ surfaces, we found that before relaxation the spin polarization of the CrAl surface is about 96% while after relaxation it decreases to about 77%.

According to figure 3, the weak CrAl surface states located in the half-metallic gap originate mainly from the p_z orbital of the surface Al and the t_{2g} orbital of the subsurface Co atoms. The Cr and Al atoms in this surface lose half of their nearest Co neighbors while subsurface Co atoms lose half of their next-nearest-neighbor Co atoms. Hence, the partial DOS of the subsurface Co is very close to the bulk DOS whereas a substantial modification is observed in the partial DOS of the surface Cr and Al atoms compared to the bulk. The lower hybridization at the surface leads to the well-known surface exchange enhancement effect visible in the increased exchange splitting of the surface Cr and Al partial DOS. This effect is more evident in the calculated atomic magnetic moments given in table 1 where, compared to the bulk values, the magnetic moment of the surface Cr atom is significantly increased and that of the surface Al atom is reversed, indicating substantial reduction of hybridization at the surface. In the minority p_z DOS of the surface Al there is a sharp peak just above the Fermi level (pertaining to some weakly coupled states) which its tail extends over the minority gap and breaks the half-metallicity of the surface. This orbital on one side points toward vacuum with no partner for coupling and hence remains narrow.

Recently it was found that the stable (001) termination of the half-metal Co_2MnSi Heusler alloy is the MnSi surface in which, similar to our case, some minority surface states break the half-metallicity [20]. They have shown that covering the surface with a pure Mn layer (substituting Si with Mn in the MnSi surface) preserves well the half-metallic character of the surface. Following this idea we substituted Al with Cr in the stable CrAl termination to obtain the modified CrCr surface. Since bulk Cr has an antiferromagnetic ground state [21], we considered both ferromagnetic and antiferromagnetic alignments of Cr moments at this modified surface. Although the calculated electronic structure indicates the half-metallic character of the ferromagnetic CrCr surface, consistent with the previous observation at the MnMn surface of Co_2MnSi, this modified surface was found to be about 3.8 eV less stable than the ideal CrAl surface. The half-metallicity of the modified CrCr termination is attributed to the presence of one extra Cr atom at the surface that compensates for lack of Co neighbors and enhances surface couplings. The antiferromagnetic state in the CrCr surface was found to be about 0.5 eV more stable than the ferromagnetic state but leads to much lower Fermi level spin polarization (about 44%).

Table 1. The atomic magnetic moments (μ_B) and the Fermi level spin polarization P (%) at the stable surface and interface. Bulk values are given for comparison. All atoms are at the surface or interface except Co atoms that are next to the surface or interface layer.

	Atomic magnetic moments					
	Co1	Co2	Cr	Al	As	P (%)
CrAl	0.90	0.90	3.57	0.10	—	77
CrAl/As (B_{Cr})	0.85	0.91	3.04	−0.16	−0.13	12
Bulk	0.93	0.93	1.83	−0.17	0	100

3.2. *Interface results*

The zinc-blende (ZB) structure of GaAs consists of Ga and As planes that are alternating in the (001) direction while, as was mentioned before, the $Co_2Cr_{0.5}Fe_{0.5}Al$ alloy has four different (001) surfaces. Therefore, at the interface of these two compounds eight ($4 \times 2 = 8$) ideal terminations are possible. All these (001) interfaces were simulated by supercell slabs containing 11 monolayers of GaAs and 9 and 11 monolayers of $Co_2Cr_{0.5}Fe_{0.5}Al$ for CrAl-and Co-terminated interfaces, respectively (depicted in figure 1). The in-plane lattice parameters of the supercell, a and b, were set to the bulk GaAs experimental lattice ($5.65\ \text{Å}/\sqrt{2}$) while the c lattice parameter and all internal atomic positions were relaxed accurately.

The interface patterns were selected in such a way that the interface Heusler atoms continue the ZB symmetry of the GaAs(001) substrate to form epitaxial interfaces. Since the interface energy mainly depends on the coupling of the interface atoms together and the subinterface layers have minor contributions to that, the relative positions of the subinterface atoms were not considered in the construction of possible interface patterns. Following these statements, the cobalt-terminated interfaces have only one possible pattern in which Co atoms sit on the bridge sites of the interface As or Ga layers[2]. Whereas for CrAl–(As, Ga) interfaces there are two possible patterns in which in one case Cr atoms continue the ZB structure of GaAs and hence it is called B_{Cr} (B denotes bridge site) while in the other one (called B_{Al}) Al atoms continue the symmetry of the substrate. In both cases the interface Cr and Al atoms sit on the bridge sites of the underlying layer (each one occupies half of the bridge sites).

For considering and comparing the stability of the different interfaces, in contrast to the surfaces, *ab initio* thermodynamics is not appropriate because there are more than two independent chemical potentials in the samples and hence several phase diagrams are required to compare the stability of the different interfaces. Therefore, instead, we calculated directly the interface energies by comparing the fully minimized total energies of the interface supercells with bulk GaAs and $Co_2Cr_{0.5}Fe_{0.5}Al$ energies. For the remaining non-stoichiometric atoms in the supercells bulk energies of

[2] For the Co–Cr/As-terminated interface, first we selected the pattern in which Co atoms continue the ZB symmetry of the substrate (similar to other Co-terminated interfaces) but after substantial efforts the required self-consistent procedure did not converge. Hence, in order to have a qualitative estimation of the stability of this interface, another pattern was adopted in which Co atoms are sitting on the hollow sites of the interface As atoms.

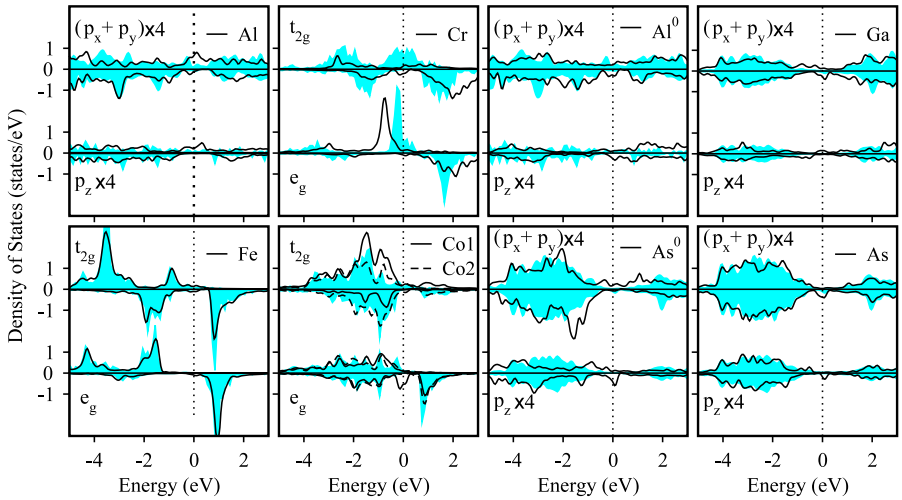

Figure 4. The spin-resolved partial DOS (see footnote 1) of the interface atoms at the B_{Cr} pattern of the CrAl/As termination. Cr, Al^0 and As^0 atoms are at the interface, Co and Ga atoms are next to the interface, and Fe, Al and As atoms are at the second layer to the interface. The plots have the same properties as PDOS plots of figure 3.

As, Al, Cr and Fe crystals were used. The results, given in table 2, show that the B_{Cr} patterns of CrAl/As is the most stable termination of this interface. It is in qualitative agreement with our surface results indicating the highest stability of the CrAl termination among $Co_2Cr_{0.5}Fe_{0.5}Al(001)$ surfaces.

After investigation of the electronic structure of $Co_2Cr_{0.5}Fe_{0.5}Al/GaAs(001)$ interfaces, we found that in all cases the Fermi level spin polarization is less than the ideal CrAl(001) surface of the Heusler alloy. Figure 4 shows the calculated DOS of the stable B_{Cr} pattern of the CrAl/As termination after projection onto the interface atomic orbitals. The calculated atomic magnetic moments out of these partial DOS are given in table 1. Comparing these partial DOS with the corresponding values at the CrAl surface (figure 4) provides useful information about interactions at this interface. The partial DOS of the interface Al, compared to the surface, show a pronounced shift toward lower energies and disappearance of all narrow peaks, indicating stronger coupling of Al atoms at the interface. This behavior is confirmed by the magnetic moment of Al at the interface that, in contrast to the surface, is very close to the bulk value (table 1). In all components of the p orbital of the interface Al, some minority interface states fill the half-metallic gap and cross the Fermi energy. In the p_z channel it seems to be due to the hybridization with interface As which is evident in the visible similarity between the partial p_z DOS of the interface As and Al atoms.

The interface Cr has a very similar e_g partial DOS to the surface while in the t_{2g} channel the density of occupied states is highly reduced. As a result, the magnetic moment of Cr at the interface is considerably lower than the surface but still much higher than the bulk value. The two cobalt atoms sitting next to the interface, in contrast to the surfaces and bulk, have different properties because one of them (Co1) is directly above the interface As while Co2 sits between two interface As atoms (bridge position). The partial DOS of Co2 is very similar to the corresponding surface and bulk DOS, showing weak interaction with the interface As atom, while the e_g orbital of Co1 effectively hybridizes with As p_z and hence some minority interface states move into the half-metallic gap of the e_g channel and reduce the Fermi level spin polarization.

Table 2. The interface energies (eV) of all possible terminations of the $Co_2Cr_{0.5}Fe_{0.5}Al(001)/GaAs(001)$ heterojunction.

Co–Cr/As	4.58[a]	Co–Cr/Ga	6.30
Co–Fe/As	1.27	Co–Fe/Ga	5.95
FeAl/As (B_{Fe})	0.15	FeAl/Ga (B_{Fe})	4.61
FeAl/As (B_{Al})	0.05	FeAl/Ga (B_{Al})	4.41
CrAl/As (B_{Cr})	−0.24	CrAl/Ga (B_{Cr})	4.82
CrAl/As (B_{Al})	0.13	CrAl/Ga (B_{Al})	4.24
$Cr^{\uparrow}Cr^{\uparrow}$/As	2.59	$Cr^{\uparrow}Cr^{\downarrow}$/As	1.69

[a] See footnote 2.

The calculated results show that the interface Ga and As atoms have small negative magnetic moments (table 1), while bulk GaAs is a nonmagnetic material. This behavior originates from the antiferromagnetic Cr–As coupling at the interface, especially in the interface pattern that the Cr–As bond has ZB geometry (B_{Cr} pattern of CrAl/As interface). First-principles studies justify the presence of a nontrivial antiferromagnetic coupling between Cr and As atoms in the artificial ZB structure of CrAs alloy[3].

It was argued that increasing Cr concentration with ferromagnetic interaction at the stable CrAl surface of $Co_2Cr_{0.5}Fe_{0.5}Al(001)$ (leading to the modified CrCr terminations) preserves the half-metallic property of the system (although it was not the stable surface). Hence, the same effect was investigated at the interface by substituting an interface Al atom with Cr at the stable ideal CrAl/As terminations to obtain the modified CrCr/As interfaces. Similar to the surface studies, both ferromagnetic and antiferromagnetic alignments of the

[3] The calculations were performed by one of the authors (SJH) by using the Pwscf package and ultrasoft GGA pseudopotentials. In this study the atomic magnetic moments of Cr and As in the ZB–CrAs alloy was found to be 3.55 μ_B and −0.56 μ_B, respectively.

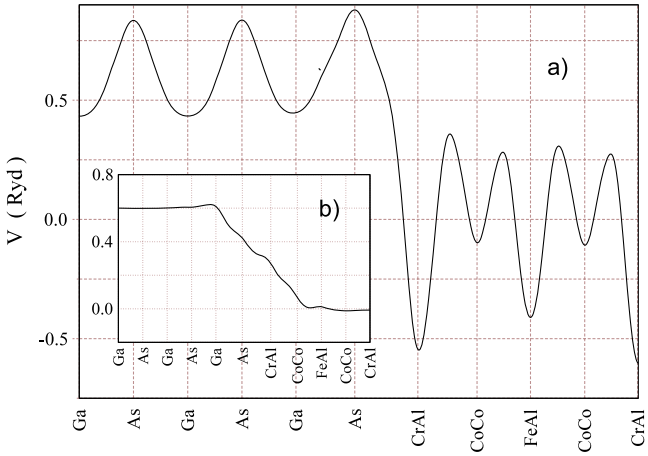

Figure 5. Total (ionic and electronic) electrostatic potential profiles of the B_{Cr} pattern of the CrAl/As interface: (a) planar average and (b) macroscopic average.

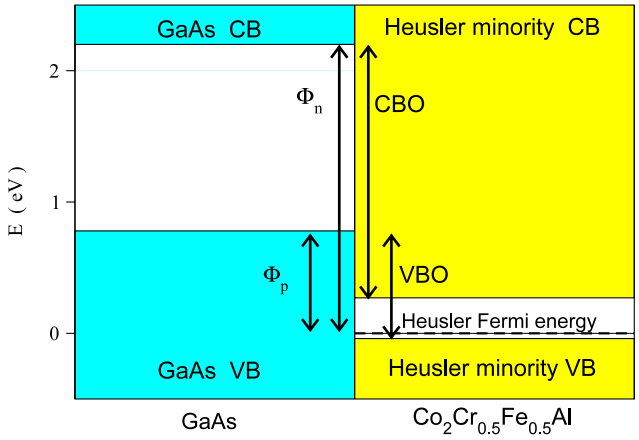

Figure 6. Schematic view of the band alignments at the $Co_2Cr_{0.5}Fe_{0.5}Al$/GaAs(001) interface with CrAl/As termination and B_{Cr} pattern. The Heusler Fermi energy (dashed line) is set to zero. VB and CB stand for valence band and conduction band, respectively.

spin moments were considered for two Cr atoms at this modified interface. After full relaxation of the corresponding supercells, we found that both $Cr^{\uparrow}Cr^{\uparrow}$/As-and $Cr^{\uparrow}Cr^{\downarrow}$/As-modified terminations are less stable than the ideal CrAl/As interfaces (see table 2). However, we calculated the electronic structure and the Fermi level spin polarization of these two modified interfaces and compared them with the B_{Cr} pattern of the ideal CrAl/As interface. It was observed that, at the $Cr^{\uparrow}Cr^{\uparrow}$/As termination, the Fermi level spin polarization is increased to about 78% while at the $Cr^{\uparrow}Cr^{\downarrow}$/As termination it is highly decreased to a negative value.

Transport properties in heterojunction devices are controlled by electronic band profiles at interfaces, so extracting band offsets in semiconductor/semiconductor and Schottky barriers in metal/semiconductor junctions are considerably important and interesting. In a half-metal the two spin channels have different characters: one is metallic while the other one is semiconducting. Hence, the half-metal/semiconductor junction in the majority channel acts as a metal/semiconductor interface while in the minority channel it behaves like a semiconductor/semiconductor junction. The valence (conduction) band offset can be written as the sum of two terms [22, 23]: the band structure contribution ΔE, which is the difference between valence (conduction) band edge energies of the two bulk materials referred to their average electrostatic potential, and the electrostatic potential line-up ΔV, due to the charge density distribution at the interface. Similarly, the ϕ_p (ϕ_n) Schottky barrier is conveniently split into two contributions: $\phi_p = \Delta E_p + \Delta V$ ($\phi_n = \Delta E_n + \Delta V$). The band structure term ΔE_p (ΔE_n) is the difference between the Fermi level of the metal and the valence (conduction) band edge of the semiconductor.

In the following we present band offsets and Schottky barriers of the B_{Cr} pattern of the CrAl/As termination. For calculating the potential line-up ΔV, first the electrostatic potential was averaged over the xy planes in the supercell $\overline{V}(z) = 1/S \int_S V(x, y, z)\,dx\,dy$ to obtain the planar average $\overline{V}(z)$. The results are plotted in figure 5 and represent two periodic functions joined smoothly at the interface. The periods of oscillations of these two functions are equal to half of the bulk lattice constants on both sides of the interface. The obvious offset of these two functions at the interface is the potential line-up ΔV. For more accurate determination of ΔV one should wash out the oscillations of $\overline{V}(z)$ by macroscopic averaging over the periods of oscillations (a):

$$\overline{\overline{V}}(z) = \frac{1}{a}\int_{z-a/2}^{z+a/2} \overline{V}(z')\,dz'.$$

The obtained macroscopic average potential which is plotted in the inset of figure 5 leads to the electrostatic potential line-up of about 8.16 eV. By using this potential line-up and bulk band structures, the minority valence band offset and the majority ϕ_p barrier were determined to be 0.82 eV and −0.78 eV, respectively. The negativity of ϕ_p comes from the fact that the valence band of GaAs lies above the Fermi level of $Co_2Cr_{0.5}Fe_{0.5}Al$ (figure 6), a phenomenon rarely observed at the metal/semiconductor interfaces. A metal–semiconductor junction should have a negative Schottky barrier if the metal has a work function (3.93 eV in our case) less than the electron affinity of the semiconductor (4.07 eV for GaAs) [24]. Such a contact would behave ohmically with a low internal resistance.

In practice it is difficult to realize such an ohmic contact, because the electronic states on the semiconductor interface pin the surface Fermi level and make the Schottky barrier less dependent on the metal work function or semiconductor electron affinity [25]. As a result, no metal has shown a negative Schottky barrier on either n-type or p-type Si [25]. But recently Tao *et al* [24] observed a negative Schottky barrier between titanium and Se-passivated n-type Si(001) and attributed it to the reduction of Si(001) surface states by thin Se layer. It seems that a similar argument is applicable to our results. Since the negative Schottky barrier in our case is observed in the majority states of the CrAl/As termination of the $Co_2Cr_{0.5}Fe_{0.5}Al$/GaAs(001) interface, hence we should

consider the majority channel. As is visible in figure 4, there is a rather small difference between the partial DOS of the interface As atom with corresponding bulk values, indicating the low intensity of the majority interface states in this system (especially around the Fermi level). It may explain the origin of the observed negative Schottky barrier in the majority channel.

Due to the well-known problem of energy bandgap underestimation, the energy values of conduction band minima are not reliable within LDA and GGA. For example, for GaAs we found a theoretical bandgap of about 0.72 eV within GGA that is almost half the experimental value (1.42 eV). This underestimation does not touch the accuracy of the minority valence band offset and the majority ϕ_p barrier but it induces substantial errors in the minority conduction band offset and majority ϕ_n barrier. Hence, in order to improve the accuracy of the last two parameters, we applied an upward shift to the conduction band of GaAs to achieve the experimental bandgap. In this way, the conduction band offset in the minority channel and ϕ_n in the majority channel were found to be about 1.93 eV and 2.20 eV, respectively.

4. Conclusions

We have investigated the electronic and magnetic properties of the $Co_2Cr_{0.5}Fe_{0.5}Al(001)$ surfaces and interfaces with GaAs(001) by using first-principles pseudopotential calculations. The results show that the CrAl surface is the most stable (001) termination of this Heusler alloy while at the interfaces with GaAs, CrAl/As termination was found to be more stable than others. It was observed that, at the stable CrAl surface, unbounded states of the surface Al destroy the half-metallic property of the system while at the interfaces, Co–As coupling is the main origin of the minority interface states in the half-metallic gap. The effects of increasing chromium concentration at the surface and interfaces on the stability, magnetic state and Fermi level spin polarization were investigated. The calculated band profile at the $Co_2Cr_{0.5}Fe_{0.5}Al(001)$/GaAs(001) interface leads to a negative p Schottky barrier for the system, indicating low internal ohmic resistance of this contact.

Acknowledgments

This work was jointly supported by the Vice Chancellor for Research Affairs of Isfahan University of Technology, Centre of Excellence for Environmental Nanotechnology, and International Centre for Theoretical Physics (ICTP) Affiliated Centre.

References

[1] Zutic I, Fabian J and Das S 2004 *Rev. Mod. Phys.* **76** 323
[2] Schmidt G and Molenkamp L W 2002 *Semicond. Sci. Technol.* **17** 310
[3] de Groot R A, Muller F M, Van Engen P G and Buschow K H J 1983 *Phys. Rev. Lett.* **50** 2024
[4] Webster P J 1971 *J. Phys. Chem. Solids* **32** 1221
[5] Buschow K H J and Van Engen P G 1981 *J. Magn. Magn. Mater.* **25** 20
[6] Galanakis I 2004 *J. Phys.: Condens. Matter* **16** 8007
[7] Galanakis I 2002 *J. Phys.: Condens. Matter* **14** 6329
[8] Nagao K, Miura Y and Shirai M 2006 *Appl. Phys.* B **73** 104447
[9] Jakob G *et al* 2005 *J. Magn. Magn. Mater.* **290–291** 1104
[10] Rata A D, Braak H, Burgler D E, Cramm S and Schneider C M 2006 *Eur. Phys. J.* B **52** 445
[11] Jones R O and Gunnarson O 1989 *Rev. Mod. Phys.* **61** 689
[12] Perdew J P, Burke S and Ernzerhof M 1996 *Phys. Rev. Lett.* **77** 3865
[13] Zhang M, Wolf A L, Zhang L, Tegus O, Bruk E, Wu G and de Boer F R 2005 *J. Appl. Phys.* **97** 10c301
[14] Baroni S, Dalcorso A, de Gironcoli S and Giannozzi P http://www.pwscf.org and http://www.quantum-espresso.org
[15] Vanderbilt D 1985 *Phys. Rev. Lett.* **32** 8412
[16] Monkhorst H J and Pack J D 1976 *Phys. Rev.* B **13** 5188
[17] Paxton A T and Methfessel M 1998 *Phys. Rev.* B **40** 3616
[18] Qian G X, Martin R M and Chadi D J 1988 *Phys. Rev.* B **38** 7649
[19] Reuter K and Scheffler M 2001 *Phys. Rev.* B **65** 035406
[20] Hashemifar S J, Kratzer P and Scheffler M 2005 *Phys. Rev. Lett.* **94** 096402
[21] Fawcett E 1988 *Rev. Mod. Phys.* **60** 209
[22] Baldereschi A, Baroni S and Resta R 1988 *Phys. Rev. Lett.* **61** 734
[23] Peressi M, Binggeli N and Baldereschi A 1998 *J. Phys. D: Appl. Phys.* **31** 1273
[24] Tao M, Udeshi D, Agarwal S, Maldonado E and Kirk W P 2004 *Solid-State Electron.* **48** 335–8
[25] Cowley A M and Sze S M 1965 Surface states and barrier height of metal semiconductor systems *J. Appl. Phys.* **36** 3212